

Raman study of the ferroelastic phase transition in $K_3Na(SeO_4)_2$

Marceli Kaczmarski and Bogusław Mróz

Institute of Physics, Adam Mickiewicz University, Umultowska 85, 61-614 Poznań, Poland

(Received 22 December 1997)

The temperature variations of both internal and external vibrations in $K_3Na(SeO_4)_2$ crystal have been observed using Raman scattering and interpreted on the basis of site-symmetry analysis. The symmetry of the intermediate phase (334–346 K) between the paraelastic $\bar{3}m$ and the ferroelastic $2/m$ phases was determined to be $\bar{3}$. Two distinct soft modes of A_g symmetry were observed in the ferroelastic phase. One of them was found to be the most intense Raman band of lattice vibrations. Its wave number fell from 36 cm^{-1} at 83 K to zero at $T_c = 334\text{ K}$, and with a critical exponent of $\frac{1}{3}$ this suggests a discontinuous character of the phase transition at T_c . From the assignment of the soft modes as librational motion of tetrahedral anions it was concluded that the ferroelastic phase transition in crystalline $K_3Na(SeO_4)_2$ is related to an ordering of orientations of these anions. Strong correlation between the deformation of tetrahedral anions and the temperature of the ferroelastic phase transition was found for different glaserite family crystals. This allowed for a prediction of a ferroelastic phase transition in $K_3Na(SO_4)_2$ to occur below 100 K. [S0163-1829(98)05618-5]

I. INTRODUCTION

Tripotassium sodium diselenate $K_3Na(SeO_4)_2$ (abbreviated as KNSe) belongs to the glaserite family crystals. The best investigated member of this family is tripotassium sodium disulphate $K_3Na(SO_4)_2$ (abbreviated as KNS).^{1–3} This family also includes $K_3Na(CrO_4)_2$ (KNCr) (Refs. 4–8) and the recently grown $K_3Na(MoO_4)_2$ (KNMo).⁹ X-ray studies have confirmed that the above compounds are isostructural. At ambient temperature the space group for the sulphate³ and chromate⁸ was established as $P\bar{3}m1$ while for the selenate¹⁰ and molybdate⁹ as $C2/c$. Moreover, the $P\bar{3}m1$ space symmetry for the selenate in the paraelastic phase, i.e., above 346 K was confirmed.¹⁰ The crystal structure of KNSe in this phase is shown in Fig. 1. In the low-temperature $C2/c$ phase, the unit cell doubles in the c direction and all atoms except Na change their sites. All oxygen atoms become inequivalent and must be numbered accordingly O(1) to O(4).

Results bearing on the KNSe crystal morphology, its thermal, dielectric, elastic, and optical properties^{11,12} as well as Brillouin scattering¹³ have proved that the crystal undergoes several phase transitions. $T_m = 1170\text{ K}$ is the melting point of the crystal. With temperature decreased below $T_1 = 758\text{ K}$ the crystal undergoes a transition from the phase of $6/mmm$ symmetry to a phase of unknown symmetry. With a further lowering of temperature, the crystal undergoes a subsequent transition at $T_2 = 730\text{ K}$ to the phase of $\bar{3}m$ symmetry. This is a trigonal prototypic phase denoted as HTP (a high-temperature phase) from which a transition to the monoclinic $2/m$ ferroelastic phase LTP (low-temperature phase) takes place. This ferroelastic phase transition is realized in two steps through an intermediate temperature phase (ITP). At $T_0 = 346\text{ K}$, the crystal symmetry decreases to $\bar{3}$ or 32, and then at $T_c = 334\text{ K}$ the crystallographic system changes from trigonal to monoclinic $2/m$. The temperature dependence of specific heat measured by differential thermal analysis and ac calorimetry reveals, at T_0 , changes characteristic of phase transitions, without temperature hysteresis effects. At the

same temperature (346 K) anomalies in the linear expansion coefficient and dielectric properties were reported.¹² Dielectric loss (tangent δ) increased monotonously with increasing temperature with no anomalies near T_0 or T_c . The temperature dependence of elastic properties of the crystal reveals anomalous changes near $T_c = 334\text{ K}$ indicating a noncontinuous character of the phase transition at this temperature. The temperature behavior of the components of the elasticity tensor was also studied for this crystal using the torsional pendulum and composite oscillator methods^{11,12} as well as from temperature studies of Brillouin scattering.¹³ The occurrence of a first-order phase transition in the crystal at about 334 K was confirmed by a change of the elementary cell parameters at this temperature established by neutron technique (Fig. 2).¹⁴

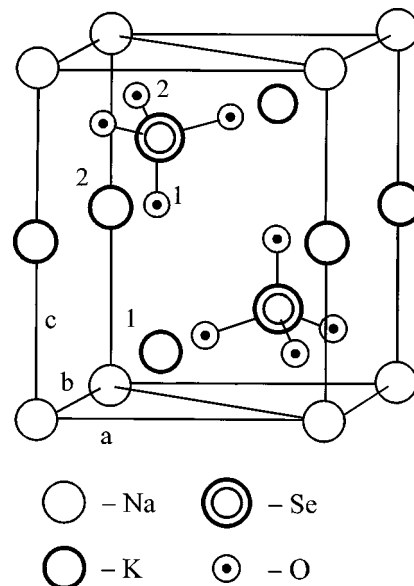


FIG. 1. Unit cell of $K_3Na(SeO_4)_2$ crystal in the paraelastic $P\bar{3}m1$ phase. Nonequivalent atoms of the same element are denoted by (1) and (2).

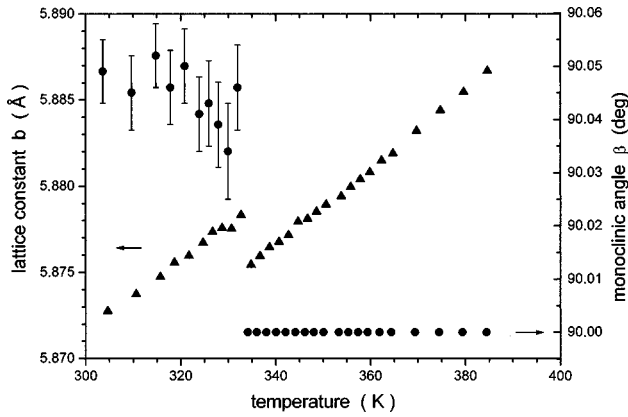


FIG. 2. Lattice constant b and monoclinic angle β vs temperature. Data were taken from neutron powder diffraction measurements (Ref. 14).

The crystal domain structure and conoscopic figures were observed for samples cut perpendicularly to the crystallographic axes. Only for samples oriented perpendicularly to the c axis were three orientational states observed in LTP, namely below T_c , and two perpendicular orientational states in ITP between T_c and T_0 . The isogyre pattern testifies to a crystal transition from uniaxial in the prototype and intermediate phase into optically biaxial in the ferroelastic phase.¹² In the same reference the intermediate phase symmetry was determined as $\bar{3}$ or 32 . However, Diaz-Hernández *et al.*¹⁵ reported that the KNSe crystal was optically biaxial in the intermediate phase and, on the basis of an analysis of the order parameter symmetry in terms of the Landau theory, they determined the symmetry of ITP as $B2/m$.

The reasons for qualitative differences in the sequences of phase transitions in the individual members of the glaserite crystal family with identical structure have not been explained satisfactorily. In the KNcr crystal a direct transition from the prototype phase $\bar{3}m$ to the ferroelastic phase $2/m$ was observed while in KNS no transition from $\bar{3}m$ to a phase of lower symmetry was detected. The symmetry of the KNSe crystal in its intermediate phase, that is, in the range 334–346 K has not been fully recognized yet. Also the mechanism of the ferroelastic phase transition on the molecular level has not been fully explained. This situation challenged us to make an attempt at determining the symmetry of the intermediate phase of $K_3Na(SeO_4)_2$ crystal and explaining the mechanism of the ferroelastic phase transition in this crystal using the method of Raman spectroscopy. Temperature investigation of Raman light scattering in crystals provides information about changes in the lattice dynamics related to phase transitions. Interpretation of these changes in terms of group theory gives insight into changes of the crystal symmetry and the molecular mechanism of phase transitions. So far the crystal of our interest has not been studied either by Raman light scattering nor infrared (IR) absorption spectroscopy. Only our earlier study¹⁶ has proved the occurrence of a strong soft mode of lattice vibration related to the ferroelastic phase transition in KNSe.

II. GROUP THEORY PREDICTIONS

There are several methods by which the number, character, and selection rules for phonons can be determined near

the Brillouin zone center, i.e., for $\mathbf{k} \cong 0$. Using the methods of site group analysis outlined for instance in Ref. 17 and the tables given therein could this be done easily and quickly. For crystals with distinguishable ionic groups, molecular site group analysis could be used giving correlation diagrams like those presented below for KNSe. The diagrams provide information necessary for the interpretation of Raman or IR spectra, in particular when structural phase transitions take place in the crystals. On the basis of a comparison of the correlation diagrams and the spectra, the postulated crystal symmetry can be verified. Moreover, some assignments of the observed modes can be made.

The KNSe crystal in HTP (prototypic paraelastic phase) belongs to the space group $P\bar{3}m1 = D_{3d}^3$. In an elementary cell of a crystal belonging to this space group the atoms or ions can take the following sites:

$$\begin{aligned} & \infty [jC_1(12)] + \infty [iC_s(6)] + \infty [(h+g)C_2(6)] + (f+e) \\ & \times C_{2h}(3) + \infty [(d+c)C_{3v}(2)] + (b+a)D_{3d}(1). \quad (1) \end{aligned}$$

The site symmetry is described using the Schoenflies notation for point groups. The symbol of a point group is followed by the number of equivalent sites (multiplicity) and preceded by a letter describing the position in the elementary cell after Wyckoff.¹⁸ For example, the notation $(f+e)C_{2h}(3)$ means that there can be three equivalent atoms (ions, nuclei) whose surroundings have C_{2h} symmetry and their positions in the elementary cell are denoted by “ e ” and/or there can be another three atoms in positions “ f ”. At the positions whose surroundings have C_n or C_{nv} symmetry there are infinitely many groups of atoms lying along a given axis, and that is why the symbols “ ∞ ” occur in Eq. (1). The positions whose surroundings have C_1 symmetry, i.e., are characterized by no symmetry are referred to as a general position. It should be emphasized that even in the general position the number of atoms n is exactly determined by the ratio of the order of the elementary cell point group and that of the site symmetry point group. Therefore, if atoms of a given kind are to occupy a general position in an elementary cell their number must be equal to the order of the point group of the elementary cell, or its multiple. It is obvious that in the $K_3Na(SeO_4)_2$ crystal of $P\bar{3}m1$ space symmetry for $Z=1$, such a situation cannot take place as there are no 12 identical atoms in the elementary cell. It should be mentioned that given the coordinates of atoms in an elementary cell their site symmetry can be found with the help of an appropriate computer program.¹⁹ Each atom or a group of n equivalent atoms of a specific site symmetry generates $3n$ normal modes. These vibrations are classified according to irreducible representations of the point group of the elementary cell.¹⁷ Table I gives a list of the vibrational modes generated by particular atoms in an elementary cell of the KNSe crystal of $P\bar{3}m1$ space symmetry, at $Z=1$. The grand total of all kinds of vibrations given in Table I must be equal to the number of degrees of freedom in a primitive cell. Obviously, vibrations of Na and K(2) atoms will not be recorded in the Raman spectra since their site symmetry D_{3d} does not generate a representation according to which at least one component of the α_{ij} polarizability tensor would transform. The number of internal vibrations can be obtained by subtracting

TABLE I. Site symmetries of atoms and the vibrational modes in the $K_3Na(SeO_4)_2$ crystal in the prototypic (paraelastic) phase.

Atom	Site symmetry	Number of vibrations					
		A_{1g}	A_{1u}	A_{2g}	A_{2u}	E_g	E_u
Na	D_{3d}				1		1
K(2)	D_{3d}				1		1
2K(1)	C_{3v}	1			1	1	1
2O(1)	C_{3v}	1			1	1	1
2Se	C_{3v}	1			1	1	1
6O(2)	C_s	2	1	1	2	3	3
Total:		$5A_{1g}$	$+A_{1u}$	$+A_{2g}$	$+7A_{2u}$	$+6E_g$	$+8E_u$

the lattice vibrations from the total number of vibrations. The lattice vibrations can be either of translational or librational character. The translational lattice modes can be determined by a method analogous to that used for the determination of the total number of modes with the only difference that the SeO_4^{2-} group should be treated as a single atom. On the basis of Table I they can be found (disregarding representations generated by all the oxygen atoms) as

$$2A_{1g} + 4A_{2u} + 2E_g + 4E_u. \quad (2)$$

The situation is different with the libration lattice modes which come only from multiatomic molecules since rotational degrees of freedom cannot be ascribed to a single atom. The librations of the SeO_4^{2-} anion whose site symmetry is C_{3v} in a cell of the point symmetry D_{3d} can be read directly from available tables:¹⁷

$$A_{1u} + A_{2g} + E_g + E_u. \quad (3)$$

Thus, the internal vibrations of a tetrahedral SeO_4^{2-} anion in the crystal studied are described by the following representations [obtained by subtraction of Eqs. (2) and (3) from the total in Table I]:

$$3A_{1g} + 3A_{2u} + 3E_g + 3E_u. \quad (4)$$

A correlation between the vibrations of free molecules (ions) and the same molecules in a crystal field of a given symmetry can be found from a correlation diagram like the one in Fig. 3. When constructing the diagram it should be remembered that for a single atom (ion) only translational degrees of freedom should be taken into account, i.e., only those irreducible representations are taken into account according to which the polar vector coordinates T_x , T_y , T_z are transformed. Vibrations of tetrahedral molecules XY_4 are usually denoted by ν_1 to ν_4 , according to the notation introduced by Herzberg.²⁰ The normal vibrations of such a molecule in a free state can be found by decomposing the reducible representation formed by a system of $3n$ Cartesian translations Γ_t into irreducible representations in the T_d point group:

$$\Gamma_t = A_1 + E + F_1 + 3F_2. \quad (5)$$

To obtain vibrations of a free molecule one should reject the representations F_1 and F_2 according to which translations and rotations of a molecule as a whole are transformed. This leaves $3n - 6$ vibrations. The analysis of vibrations of a molecule (ion) in a crystal elementary cell demands taking into

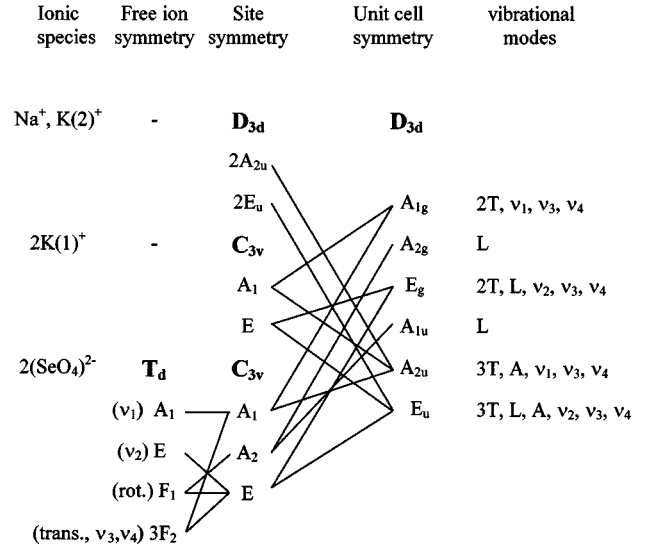


FIG. 3. Correlation diagram for $K_3Na(SeO_4)_2$ crystal in the prototypic $P\bar{3}m1 \equiv D_{3d}^3$ phase. T , L , and A denote translational, librational, and acoustic modes, respectively.

account all representations from Eq. (5) since the translations and rotations of a free multiatom ion become translational and librational lattice modes.

A similar analysis can be made for ITP although x-ray structural data for this crystal phase are unavailable. This phase (334 to 346 K) has been postulated to have point symmetry $\bar{3}$ or 32 (Refs. 11 and 12) or $B2/m$.¹⁵ Assuming that KNSe in the intermediate phase has space symmetry $P321 \equiv D_3^2$, the atoms (ions) can occupy the following sites:

$$\begin{aligned} &\infty[gC_1(6)] + \infty[(f+e)C_2(3)] + \infty[(d+c)C_3(2)] \\ &+ (b+a)D_3(1). \end{aligned} \quad (6)$$

The only possible arrangement of site symmetry of atoms in the elementary cell (assuming $Z=1$) is as follows: Na and K(2) at $D_3(1)$ site, 2K(1), 2Se and 2O(1) at $C_3(2)$ sites and the other 6 O(2) oxygen atoms at $C_1(6)$ sites. These sites generate the following representations:

$$6A_1 + 8A_2 + 14E. \quad (7)$$

Among them A_1 vibrations are active in the Raman spectra, A_2 in IR absorption spectra, and E vibrations in both kinds of spectra.

If the crystal symmetry of ITP is described by the space group $P\bar{3} \equiv S_6^1$, the possible sites in an elementary cell are

$$\begin{aligned} &\infty[gC_1(6)] + (f+e)C_i(3) + \infty[(d+c)C_3(2)] \\ &+ (b+a)S_6(1). \end{aligned} \quad (8)$$

This leads to the following normal vibrations:

$$6A_g + 8A_u + 6E_g + 8E_u. \quad (9)$$

The modes A_g and E_g are Raman active while A_u and E_u are IR active. The correlation diagrams for both postulated crystal symmetries in ITP are given in Figs. 4 and 5.

At 334 K, on transition from the intermediate to the ferroelastic phase the elementary cell symmetry is rapidly re-

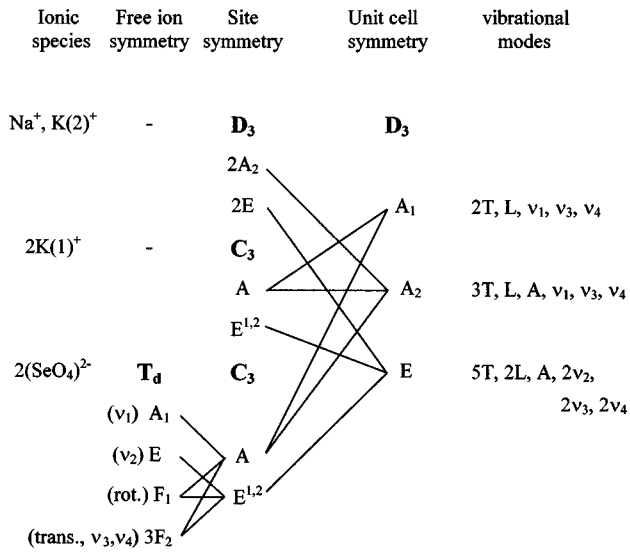


FIG. 4. Correlation diagram for $K_3Na(SeO_4)_2$ crystal in the intermediate $P321 \equiv D_3^2$ phase.

duced and its volume becomes four times increased. In the latter phase the space symmetry group of the crystal is $C2/c = C_{2h}^6$ and an elementary cell comprises four structural units ($Z=4$). This group admits of the following site symmetries:

$$\infty[fC_1(8)] + \infty[eC_2(4)] + (d+c+b+a)C_i(4). \quad (10)$$

Keeping in mind that, here, the volume of the primitive cell is one half of that of the elementary cell, the total number of modes is

$$19A_g + 22A_u + 20B_g + 23B_u. \quad (11)$$

The A_g and B_g are Raman active while A_u and B_u are IR-active modes. The correlation diagram for the ferroelastic phase is given in Fig. 6. All the correlation diagrams presented above will be discussed in Sec. IV.

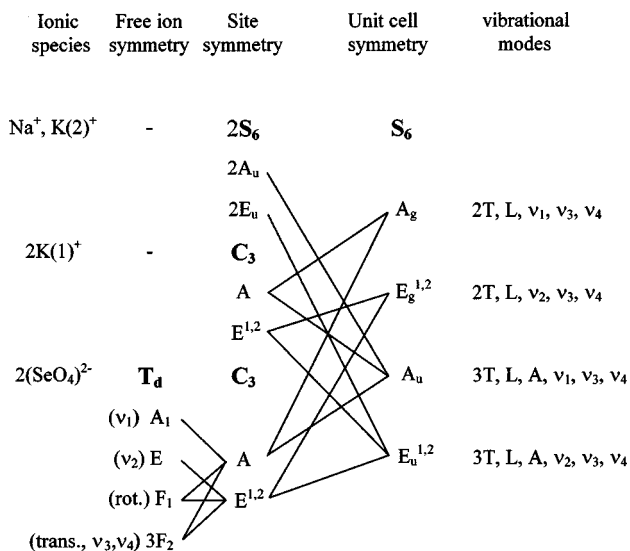


FIG. 5. The same diagram as in Fig. 4 but assuming the $P\bar{3} \equiv S_6^1$ (Ref. 1) symmetry.

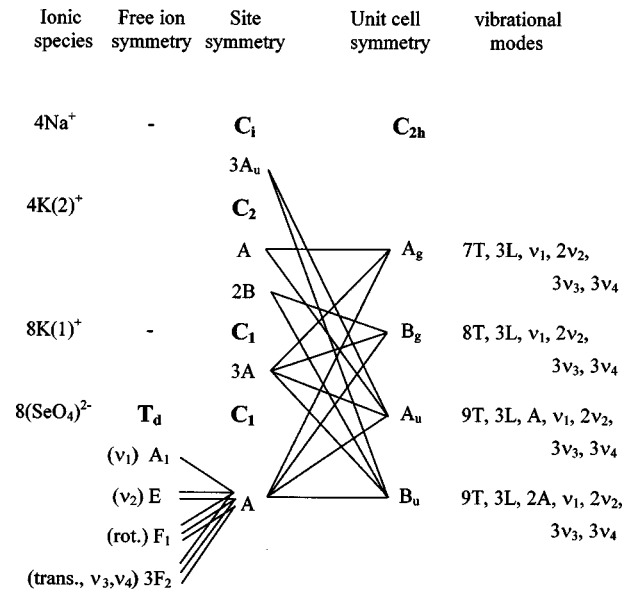


FIG. 6. Correlation diagram for $K_3Na(SeO_4)_2$ crystal in the ferroelastic $C2/c \equiv C_{2h}^6$ phase.

III. EXPERIMENTAL

A. Samples

KNSe crystals were grown from a saturated stoichiometric solution of sodium and potassium hydroxides and selenium acid by the dynamic method at a constant temperature of 300 K. The product of synthesis was recrystallized from the appropriate solution, made using distilled water. The single crystals obtained were of good optical quality, colorless, and transparent in the shape of a prism with hexagonal base and an edge length from 5 to 20 mm. Their density was determined as $3.15 \pm 0.01 \text{ g/cm}^3$, and their chemical composition was verified spectroscopically. The c -axis direction was assumed as the direction perpendicular to the hexagonal base, the b axis was assumed to coincide with the longer diagonal of the base, and the a axis direction was assumed as perpendicular to the b and c axes. Samples to be studied were cut out as rectangular parallelepipeds $4 \times 5 \times 6 \text{ mm}^3$ in size with edges parallel to either of the crystallographic axes a , b , or c .

B. Raman spectra

The Raman spectra presented in this work were obtained on a double-grating Raman spectrometer JEOL JRS-S1 coupled to a PC via a programmable Computer Interface Module Model SR-254 Stanford Research System. The wave number accuracy was $\pm 1 \text{ cm}^{-1}$ and reproducibility $\pm 0.3 \text{ cm}^{-1}$. Survey Raman spectra in the range from 0 to 1000 (or 250–1250) cm^{-1} were recorded with the use of a 6 cm^{-1} entrance slit when single crystals or liquids were studied and a 3.4 cm^{-1} entrance slit for the study of powders. Lattice vibrations in the range below 250 cm^{-1} and temperature variations in individual bands in the spectra were recorded for a slit width of 1.7 cm^{-1} . The sensitivity of the spectrometer was varied in the range from 10 000 (survey spectra of single crystals) to the maximum value of 250 pulses/sec when taking spectra of solutions. Depending on

the above parameters the spectra were recorded at a rate varying from 5 to 100 $\text{cm}^{-1}/\text{min}$. Time constants were selected automatically.

The Raman spectra were excited by the 488.0 nm line of argon ion laser radiation. The power of the exciting radiation measured at the site of the sample was of about 50 mW. The use of an interference filter in order to avoid plasma line recording proved necessary only when studying powder samples. Raman spectra were recorded in the direction perpendicular to that of the exciting beam. The spectra of polycrystalline samples were obtained by the reflection method. In this method the exciting beam made a small angle with the surface of the sample pressed into a hollow in a metal powder holder, and the scattered radiation was recorded perpendicularly to the exciting beam. The spectra of water solutions of the crystals, at a few percent concentration, were taken using standard quartz cuvettes. For temperature measurements in the range 80–380 K we used a cryostat made at our laboratory that ensured temperature stabilization and measurement with an accuracy of ± 0.06 K.

IV. RESULTS AND DISCUSSION

As shown in Sec. II, reduction of the crystal symmetry is accompanied by an increasing number of normal modes. Their total number increases from 42 in the prototype and intermediate phases to 84 in the ferroelastic phase. The number of Raman-active modes increases by then from 17 in 3 m HTP to 18 in $\bar{3}$ or to 34 in 32 ITP and to 39 in $2/m$ LTP. For the sake of clarity, our discussion of the Raman spectra obtained is divided into two parts concerning external and internal vibrations respectively.

A. External modes

From a comparison of the correlation diagrams presented in Sec. II, it is easy to notice that in the high temperature D_{3d} phase only five modes are predicted to appear in the Raman spectra in the low-frequency external vibrations region. They are two lattice vibrations of translational character related to the motion of $K(1)$ and SeO_4 ions of both A_{1g} and E_g symmetry and one of librational character of the tetrahedral group of symmetry E_g . In the ITP, if the crystal symmetry is lowered to S_6 , only one mode more could be recorded of A_g symmetry. This is the libration of the SeO_4 ion with a wave number of about 60 cm^{-1} (Fig. 7). The assignment of all external vibrations could be performed easily for HTP. The two A_{1g} modes with wave numbers 162 and 89 cm^{-1} (Fig. 7) must belong according to the correlation diagram (Fig. 3) to translations of $K(1)$ and SeO_4 ions respectively (for translatory modes their frequency depends on the mass of the vibrating units). The E_g translations of these ions appeared at about 156 and 105 cm^{-1} , respectively, (Figs. 8 and 9). The band at 60 cm^{-1} in Fig. 9 must be the librational E_g mode of the tetrahedral group.

Seven translational and three modes of librational nature of A_g symmetry could be identified for LTP. At liquid N_2 temperature the motion of K gives rise to the bands at 174, 153, 143, and 136 cm^{-1} while translations of SeO_4 —to 129, 110, and 97 cm^{-1} Raman bands. Librations could be seen at 28, 36, and $61\text{--}65 \text{ cm}^{-1}$ (Figs. 7, 8, and 10). Splitting of the

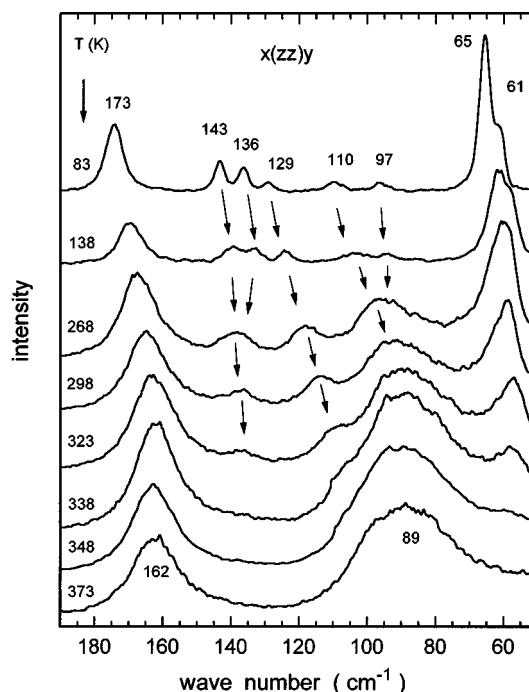


FIG. 7. Evolution of Raman lattice vibrations spectrum in the $x(zz)y$ scattering geometry. The very strong soft mode lying below 50 cm^{-1} is presented in a separate figure.

band at about 60 cm^{-1} is caused by the domain structure of the sample. Because of the low intensity it was not possible to identify all B_g modes in LTP. Three librations appeared with wave numbers 28, 36 and 71 cm^{-1} . Only four of the eight translational modes could be seen in Fig. 9. There are three $K(1)$ or $K(2)$ vibrations with wave numbers 174, 154, and 136 cm^{-1} and a SeO_4 translational mode at 125 cm^{-1} .

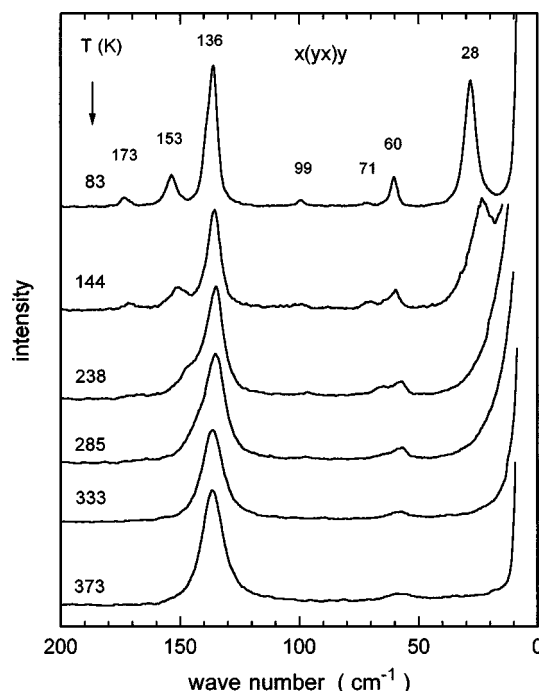


FIG. 8. Raman spectra of lattice vibrations in the $x(yx)y$ geometry for different temperatures. Modes of A_g symmetry become of E_g symmetry above $T_c = 334 \text{ K}$.

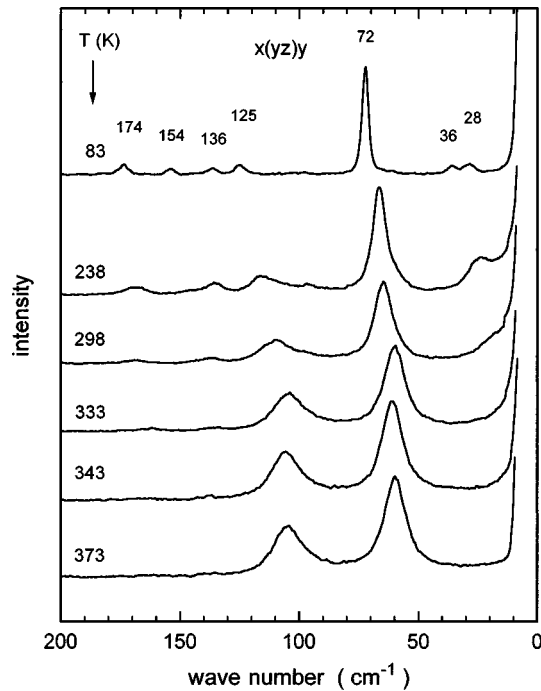


FIG. 9. Raman spectra of lattice modes of B_g (below T_c) and of E_g (above T_c) symmetry of $K_3Na(SeO_4)_2$ crystal for different temperatures, obtained in the $x(yz)y$ scattering geometry.

The temperature variations of the wave numbers of lattice vibrations recorded in the $x(zz)y$ scattering geometry are depicted in Figs. 11 and 12, where the frequencies versus temperature for some of the modes could be approximated by polynomials of the first, second, or third degree. Analysis of the behavior of $\tilde{\nu}_i(T)$ functions reveals their changes not

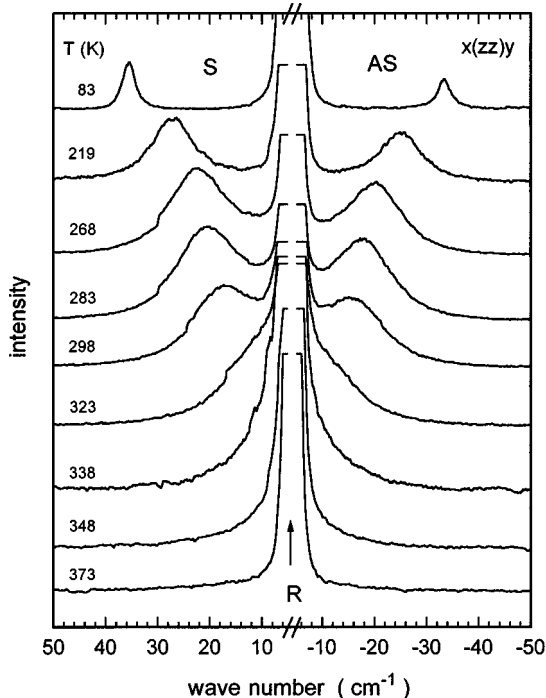


FIG. 10. Raman spectra of the soft mode in $K_3Na(SeO_4)_2$ crystal for different temperatures. The $x(zz)y$ scattering geometry was used.

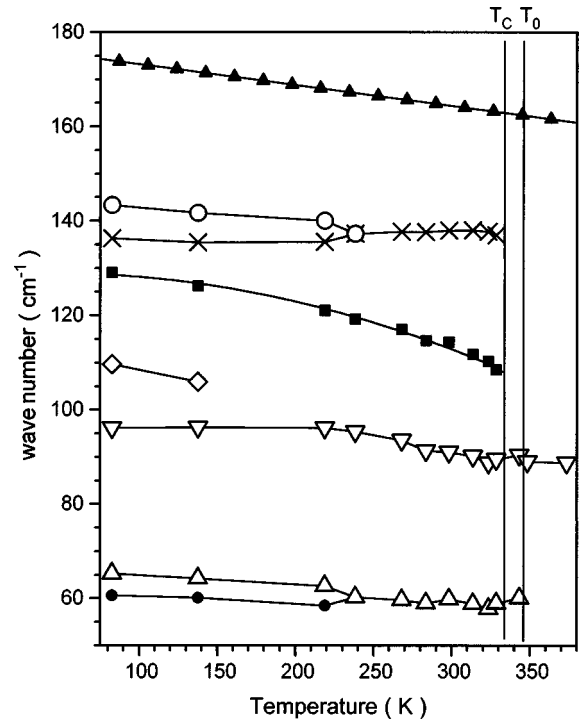


FIG. 11. Temperature dependences of wave numbers of the modes depicted in Fig. 7.

only at T_0 and T_c but also near 240 K. At this temperature some anomalies have been detected by dielectric measurements for multidomain samples.²¹

The soft mode presented in Fig. 10 is the strongest lattice mode in the Raman spectra at liquid nitrogen temperature. Its maximum intensity is over two times greater than that of the band at 65 cm^{-1} (Fig. 7). The wave number of this mode decreases to zero at T_c at rising temperature and the half width increases then as shown in Fig. 12. The critical behavior of this vibration could be described by $\omega \sim (T - T_c)^{1/3}$ in a wide temperature range (Fig. 13). The value $\frac{1}{3}$ of the critical exponent suggests a first-order character of the phase transition at T_c . Much the same soft mode was observed in the K_2SeO_4 crystal.²² A second soft mode of the same A_g

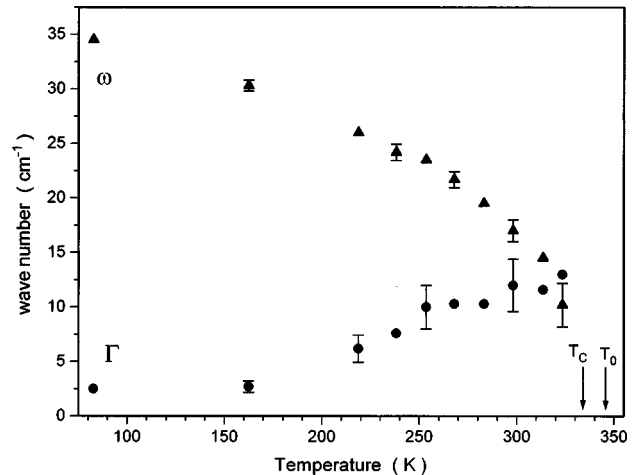


FIG. 12. Wave number ω and FWHH (full width at half height) Γ of the soft mode observed in $x(zz)y$ geometry as a function of temperature.

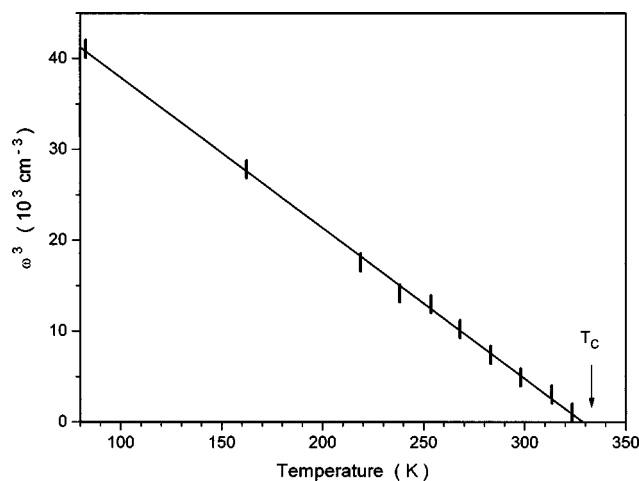


FIG. 13. Temperature dependence of the frequency of the soft mode from Fig. 10. The relation: $\omega = (T_c - T)^{1/3}$ suggests a first-order phase transition at $T_c \approx 334$ K.

symmetry and similar phenomena could be observed in another scattering geometry (Fig. 8). However, because of its lower frequency and intensity it is masked by a Rayleigh line at temperature higher than 250 K. As we have explained earlier, both of the soft modes are connected to librational motions of tetrahedral SeO_4 anions.

B. Internal modes

The Raman spectra of internal vibrations in the KNSe crystal are shown together with the spectra of two other isostructural crystals: KNCr and KNS in Fig. 14. All spectra were taken for powdered samples at room temperature. The spectra of the selenate and chromate are similar although

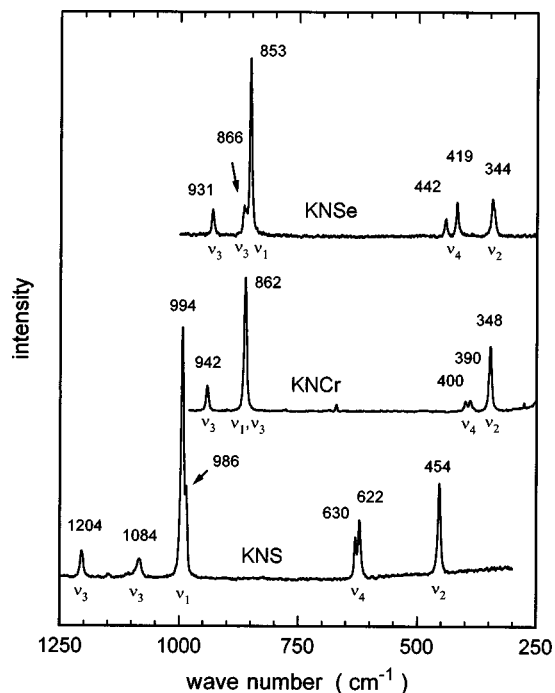


FIG. 14. The Raman spectra of internal vibrations of three glaserite family crystals. The spectra were taken for powdered samples.

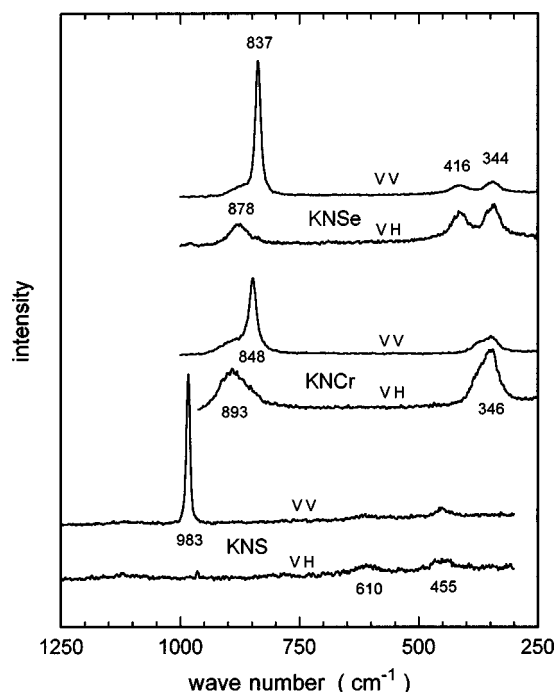


FIG. 15. The Raman spectra of water solutions of the same crystals as in Fig. 14. The VH spectra were taken at twice (for KNS) and four times (for other crystals) higher sensitivity than that at which their VV spectra were taken.

these crystals were in different phases, ferroelastic and paraelastic, respectively. The shift of the frequency of vibrations for the sulphate can be explained by shorter interatomic distances and increased force constants in this crystal. Indeed, an increase in Raman frequencies by about 100 cm^{-1} was observed in the spectra of KNCr and KNS crystals subjected to a pressure of over 20 GPa, inducing a reduction of interatomic distances.²³

Certain information on the nature of bonds in a given crystal can be inferred from a comparison of the internal vibrations frequency measured in the crystal and in its water solution. Ethier *et al.*²⁴ noted that the vibration frequencies of the tetrahedral anion SeO_4^{2-} in Cs_2SeO_4 crystal are by about 1.5% lower than the corresponding frequencies of this anion in water solution. Such a softening of the modes was accounted for as a result of a weakening of the ionic character of the bonds in the crystal caused by a shift of part of the electric charge from the tetrahedron to Cs^+ cations or to any other place in the elementary cell. A comparison of the spectra from Figs. 14 and 15 suggests that in $\text{K}_3\text{Na}(\text{SeO}_4)_2$ crystal the situation is the reverse as the frequency of vibrations in the crystal is by about 2% higher (for the ν_1 mode). This would mean that the ionic character of the bonds increases in the crystal due to charge transfer from the surroundings to the tetrahedron. The most probable charge donor is a slightly bonded $\text{K}(2)^+$ cation.

In the Figs. 16–18 we present the internal modes of KNSe detected at different temperatures. As it is evident the transition from the paraelastic high-temperature phase to the intermediate phase does not affect the spectra significantly. The number of modes increases when the crystal is cooled and the phase transition to the low-temperature ferroelastic

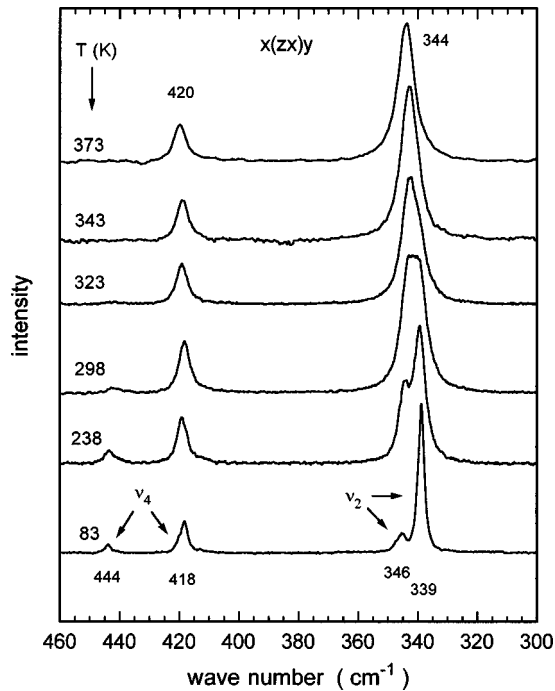


FIG. 16. The Raman spectra of internal ν_2 and ν_4 vibrations in $K_3Na(SeO_4)_2$ crystal for different temperatures obtained in the $x(zx)y$ scattering geometry.

phase takes place. The results obtained are in good agreement with the correlation diagrams given in Figs. 3, 5, and 6 (Sec. II).

The existing assignment for the symmetry of the intermediate phase points to $\bar{3}$, 32 (Refs. 11 and 12) and recently to a mixture of two monoclinic phases.¹⁵ Let us assume that ITP has point symmetry $32 (D_3)$. In this case the number of

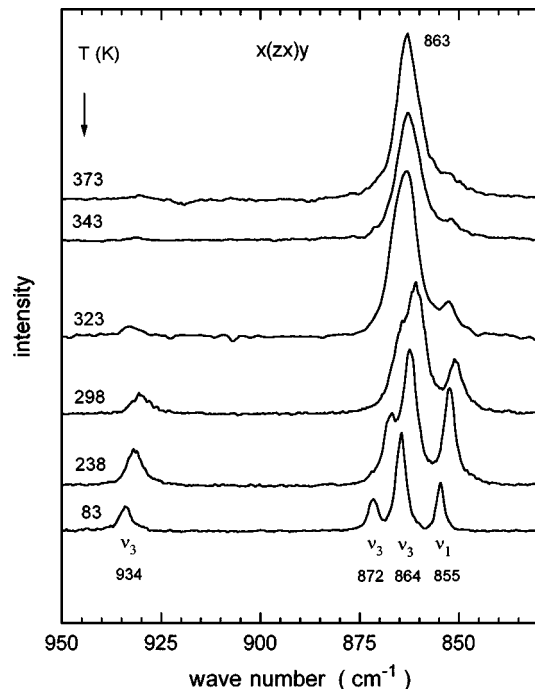


FIG. 17. The Raman spectra of internal ν_1 and ν_3 vibrations in $K_3Na(SeO_4)_2$ crystal for different temperatures in the $x(zx)y$ scattering geometry.

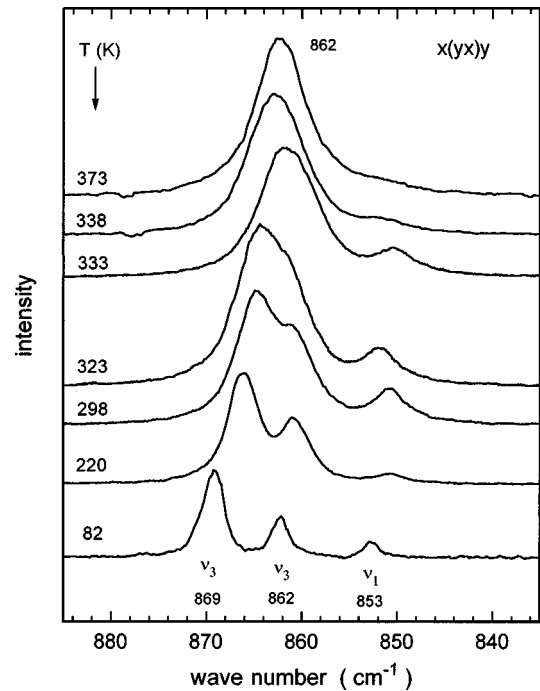


FIG. 18. The Raman spectra of $K_3Na(SeO_4)_2$ crystal for different temperatures in the wave number range of $830\text{--}890\text{ cm}^{-1}$ obtained in the $x(yx)y$ scattering geometry.

Raman-active nonfully symmetric internal vibrations would be twice higher in ITP than in HTP (compare the diagrams given in Figs. 3 and 4). Moreover, one could expect a splitting between longitudinal and transverse polar modes. This is not our case. Our results are also in contradiction to the model proposed by Diaz-Hernández *et al.*¹⁵ where monoclinic symmetry of ITP is proposed. Such symmetry would lead to significant differences between the spectra collected in HTP and ITP. Considering all the above remarks, we may conclude that the symmetry of the intermediate phase of KNSe is trigonal with the point group $\bar{3}$.

C. Mechanism of the ferroelastic phase transition

Results of the Raman-scattering studies show that the mechanism leading to the ferroelastic phase transition in the $K_3Na(SeO_4)_2$ crystal resides in the ordering of orientations of the tetrahedral anions SeO_4^{2-} . This process is realized in two stages. The transition from the prototype phase to the intermediate phase at $T_0 = 346\text{ K}$ is related to a deviation of the direction of the Se and O(1) bond from parallel to the c axis of the elementary cell (Fig. 1). This deviation grows with decreasing temperature of the crystal and is manifested by a gradual increase in intensity of the band related to the librations of the tetrahedra at about 60 cm^{-1} . The splitting of the band into two components described at liquid-nitrogen temperature by wave numbers of 61 and 65 cm^{-1} (Fig. 7) as well as the presence of two directions of domain orientations observed in ITP suggests that the deviation of the Se-O bond may occur along two mutually perpendicular directions with a certain statistical distribution. The phase transition ITP \rightarrow LTP at about 334 K may be explained by hindering of the tetrahedron rotations about the threefold symmetry axis. The oxygen atoms O(2), O(3), and O(4) are bound in poten-

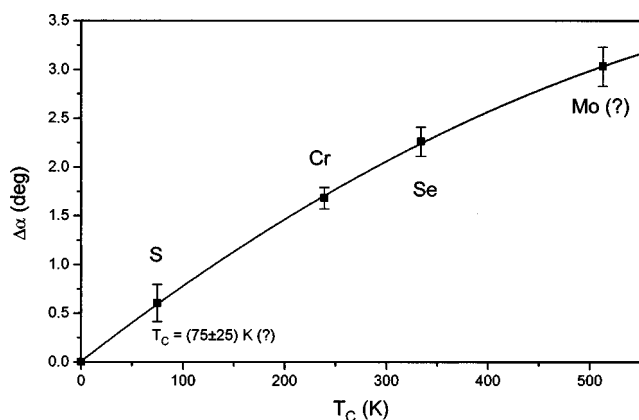


FIG. 19. Correlation between the deformation of tetrahedral XO_4^{2-} anions (where $X = S, Cr, Se, \text{ or } Mo$) and ferroelastic phase-transition temperatures in glaserite family crystals. See the discussion in the text.

tial wells that are deeper the lower the crystal temperature, and the tetrahedra rotations are restricted to librations observed as soft modes at 36 and 28 cm^{-1} at about 80 K.

If the ordering in orientation of the tetrahedral anions leads to the ferroelastic phase transition the question arises why in isostructural $KNCr$ the phase-transition temperature is much lower (239 K), in $KNMo$ much higher (513 K), and in KNS no transition was observed in the temperature range studied from 100 to 1350 K. The answer follows from a comparison of the degree of deformation of individual tetrahedra. According to the model proposed, it can be expected that the greater the deviation of the oriented anions from the ideal tetrahedron the easier is the ordering of their orientations against the disturbing thermal motions. Let the difference from ideal symmetry in HTP reside in a difference between the angles O_1BO_2 and O_2BO_2 , where: $B = S, Cr, Se, \text{ or } Mo$. Denoting this difference by $\Delta\alpha$, an approximately linear dependence between the degree of tetrahedra deformation and the phase-transition temperature T_c is obtained, for different glaserite structure crystals. A more precise fitting could be made using a polynomial of the second degree with a small quadratic term (Fig. 19). For the $KNMo$ crystal struc-

tural data are available only for LTP, so the values of the appropriate angles are replaced by mean values and the result is decreased by 20% (in analogy to $KNSe$). The missing phase-transition temperature for the KNS crystal can be read from the diagram and its surprisingly low value explains why no ferroelastic phase transition has been observed in KNS in the studies performed so far above 100 K.

V. CONCLUSIONS

The results of our temperature Raman light scattering studies performed for the $K_3Na(SeO_4)_2$ crystal have led to the following conclusions:

(i) Critical changes in the Raman spectrum were detected both at the prototype to intermediate phase transition temperature $T_0 = 346$ K and at the ferroelastic phase transition ($T_c = 334$ K).

(ii) In the intermediate phase the crystal has the point symmetry $\bar{3}$.

(iii) The ferroelastic phase transition at $T_c = 334$ K is related to a softening of two external vibrations of A_g symmetry and wave numbers of about 36 and 28 cm^{-1} (at 83 K).

(iv) The wave number of the soft mode of 36 cm^{-1} decreases with a critical exponent $\frac{1}{3}$, which suggests that the ferroelastic phase transition is of first order.

(v) Identification of the lattice soft mode of very high intensity as librations of the tetrahedral SeO_4^{2-} anion and its critical behavior at T_c indicates the ordering of the tetrahedra orientations as the mechanism leading to the ferroelastic phase transition in $KNSe$.

(vi) A comparison of the structures of different glaserite family crystals and their temperatures of the ferroelastic phase transitions justifies the hypothesis that T_c is higher the greater the deformation of the tetrahedral molecules. The structure of the SO_4 group close to the ideal tetrahedron explains the fact that no ferroelastic phase transition has hitherto been observed in KNS above 100 K.

ACKNOWLEDGMENT

The authors wish to thank Professor T. Krajewski for many helpful discussions.

¹M. E. Hilmy, *Am. Mineral.* **38**, 118 (1953).

²W. Eysel, *Am. Mineral.* **58**, 736 (1973).

³K. Okada and J. Osaka, *Acta Crystallogr., Sect. B: Struct. Crystallogr. Cryst. Chem.* **36**, 919 (1980).

⁴A. Goldberg, W. Eysel, and T. Hahn, *Neues Jahrb. Mineral. Monatsh.* **6**, 241 (1973).

⁵T. Krajewski, B. Mróz, P. Piskunowicz, and T. Bręczewski, *Ferroelectrics* **106**, 225 (1990).

⁶B. Mróz, H. Kiefte, M. J. Clouter, and J. A. Tuszynski, *Phys. Rev. B* **43**, 641 (1991).

⁷J. Fábry, T. Bręczewski, and G. Madariaga, *Acta Crystallogr., Sect. B: Struct. Sci.* **50**, 13 (1994).

⁸G. Madariaga and T. Bręczewski, *Acta Crystallogr., Sect. C: Cryst. Struct. Commun.* **46**, 2019 (1990).

⁹J. Fábry, V. Petříček, P. Vaněk, and I. Císařová, *Acta Crystallogr., Sect. B: Struct. Sci.* **53**, 596 (1997).

¹⁰J. Fábry, T. Bręczewski, and V. Petříček, *Acta Crystallogr., Sect. B: Struct. Sci.* **49**, 826 (1993).

¹¹T. Krajewski, P. Piskunowicz, and B. Mróz, *Phys. Status Solidi A* **135**, 557 (1993).

¹²T. Krajewski, P. Piskunowicz, and B. Mróz, *Ferroelectrics* **159**, 161 (1994).

¹³B. Mróz, H. Kiefte, M. J. Clouter, and J. A. Tuszynski, *Phys. Rev. B* **46**, 8717 (1992).

¹⁴S. Kim, Chalk River Laboratories, Canada, Annual Report (1995).

¹⁵J. Diaz-Hernández, J. L. Mañes, M. J. Tello, A. López-Echarri, T. Bręczewski, and I. Ruiz-Larrea, *Phys. Rev. B* **53**, 14 097 (1996).

¹⁶M. Kaczmarek, B. Mróz, H. Kiefte, M. J. Clouter, and N. H. Rich, *Ferroelectrics* **152**, 331 (1994).

¹⁷D. L. Rousseau, R. P. Bauman, and S. P. S. Porto, *J. Raman Spectrosc.* **10**, 253 (1981).

- ¹⁸*International Tables for X-ray Crystallography* (Kynock, Birmingham, UK, 1952).
- ¹⁹GSAS—General Structure Analysis System, R. B. Von Dreele and A. C. Larson (computer program from Los Alamos server), University of California (1995).
- ²⁰G. Herzberg, *Molecular Spectra and Molecular Structure: II Infra-Red and Raman Spectra of Polyatomic Molecules* (Van Nostrand, Princeton, NJ, 1945).
- ²¹S. Mielcarek and B. Mróz (unpublished).
- ²²C. Caville, V. Fawcett, and D. A. Long, in *Proceedings of the 8th International Conference on Raman Spectroscopy*, edited by E. D. Schmid (Schulz, Freiburg, 1976).
- ²³F. E. Bernardin III and W. S. Hammack, *Phys. Rev. B* **54**, 7026 (1996).
- ²⁴L. Ethier, N. E. Massa, A. Béliveau, and C. Carlone, *Can. J. Phys.* **67**, 657 (1989).